

# Effect of Internal Mass Isolation on the Radiated Sound Power of a Submerged Hull

H. Peters (1), R. Kinns (1), N. Kessissoglou (1) and S. Marburg (2)

(1) School of Mechanical and Manufacturing Engineering, The University of New South Wales, Sydney, NSW 2052, Australia

(2) LRT4 – Institute of Mechanics, Universität der Bundeswehr München, D-85579 Neubiberg, Germany

## ABSTRACT

The primary aim of machinery isolation in submarines is to isolate structural vibration of the onboard machinery from the hull and to reduce far-field radiation of noise from the submarine. The isolation system can also be used to protect sensitive components from underwater explosions. A substantial proportion of the total submarine mass is on flexible mounts that isolate supported masses from the hull at frequencies above the mounting system resonant frequency. This reduces the dynamically effective mass of the hull and affects the signature of the submarine due to propeller excitation. A fully coupled finite element / boundary element (FE/BE) model has been developed to investigate the effect of system isolation in a submarine hull. The finite element model of the structure includes internal structures to represent the machinery and other flexibly mounted components. Sound power plots demonstrate the effect of machinery isolation on the acoustic signature of a submarine due to excitation from its propeller.

## INTRODUCTION

In the unclassified literature, simplifying approaches to model the internal mass distribution of a submarine have considered the internal masses as either evenly distributed over the pressure hull (Pan et al., 2008; Caresta and Kessissoglou, 2009) or placed in the form of rigidly attached lumped masses at the ends of the hull (Merz et al., 2009). Such low frequency analytical and 2D computational models to predict the structural responses and radiated sound fields of a submarine are restricted due to mathematical complexity and are unable to consider realistic internal mass representation. 2D axi-symmetric models are restricted to axi-symmetric mass distributions which does not allow for discrete masses. Analytical models are in theory capable of more complex mass distributions but the mathematical complexity usually limits their internal mass distributions similarly as in 2D axi-symmetric models. 3D computational models do not suffer such restrictions and it is possible to model complex geometries and more realistic internal mass distributions (Miller, 2001).

In order to accurately model the interior mass in a submarine, it is important to consider both the mass distribution and its attachment to the pressure hull. For example, there are different ways to mount the propulsion system, which accounts for a major proportion of the total mass of a submarine. Nuclear-powered submarines may use a propulsion arrangement that includes turbines, gearboxes and other systems in a large structure on soft mounts. Details are not published in the open literature, but arrangements of this type have also been used for surface ships (Kinns and Faulder, 1992). Other arrangements may include high-speed electric motors, gearboxes and generators on soft mounts. Alternatives include heavy, low-speed electric motors that are connected directly to the hull. There are trade-offs between the various types of arrangements in terms of cost and overall acoustic performance. The effect of machinery layout choice on sound radiation due to the propeller is part of that evaluation process. Furthermore, a large proportion of the total mass of diesel-electric and fuel cell submarines is taken up by batteries required to store electric energy. Batteries may also be mounted flexibly on the pressure hull in order to protect them from shock due to underwater explosions.

In this work, a fully coupled 3D finite element/boundary element (FE/BE) model of a simple fluid-loaded cylindrical shell closed by hemispherical end caps and with internal masses is

developed. The effects of the mass distribution and the flexibility of the mounting arrangement on the radiated sound power are discussed.

## NUMERICAL MODEL OF SUBMERGED HULL

A fully coupled FE/BE model of a simplified physical model of a submarine was developed as follows. A cylinder with hemispherical end caps was used to represent the pressure hull. The hemispherical end caps were chosen for simplicity. The hull is separated into three equal compartments by two internal bulkheads. The structural model was modelled in ANSYS (ANSYS, 2009) and has 4992 quadratic finite shell elements (Shell 281). The internal masses are modelled as independent spring-mass systems distributed evenly over the three compartments of the pressure hull. At each designated attachment location, two spring-mass systems are placed - a flexible spring-mass system and an almost rigid spring-mass system. For simplicity, this quasi-rigid spring is preferred over an entirely rigid connection. Furthermore, this combination of flexible and rigid spring-mass systems allows for various degrees of flexibility of the mounting arrangement. Figure 1 illustrates the design of the dual spring-mass system. The mass  $m$  of the spring-mass system can be shifted between the flexible and rigid sides.  $\delta$  is the mass distribution factor. The stiffness  $k_1$  on the flexible side is adjusted such that the eigenfrequency is kept constant at 5 Hz. The stiffness  $k_2$  on the rigid side is arbitrarily chosen so that the eigenfrequency is 500 Hz which is well above the highest frequency of 100 Hz considered in this work. The stiffness of the springs are the same in the  $x$ ,  $y$  and  $z$  directions. Three spring-mass systems are attached to each ring stiffener as shown in Figure 2 and there are 14 ring stiffeners in each compartment. Hence, a total of 126 spring-mass systems are modelled. Figure 3 shows the distribution of the spring-mass systems along the pressure hull.

The water surrounding the hull was modelled using the non-commercial code AKUSTA (Marburg and Schneider, 2003; Marburg and Amini, 2005). The boundary element model has 576 linear discontinuous boundary elements. The structure and fluid subdomains were fully coupled and the resulting system of equations for the submerged structure is given by (Peters et al., 2012)

$$\begin{bmatrix} \mathbf{K} - i\omega\mathbf{D} - \omega^2\mathbf{M} & -\mathbf{C}_{sf} \\ -i\omega\mathbf{G}\mathbf{C}_{fs} & \mathbf{H} \end{bmatrix} \begin{bmatrix} \mathbf{u} \\ \mathbf{p} \end{bmatrix} = \begin{bmatrix} \mathbf{f}_s \\ \mathbf{f}_f \end{bmatrix}. \quad (1)$$

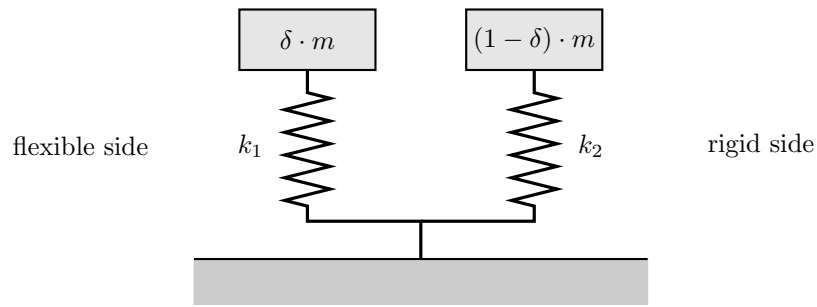


Figure 1. Dual spring-mass system

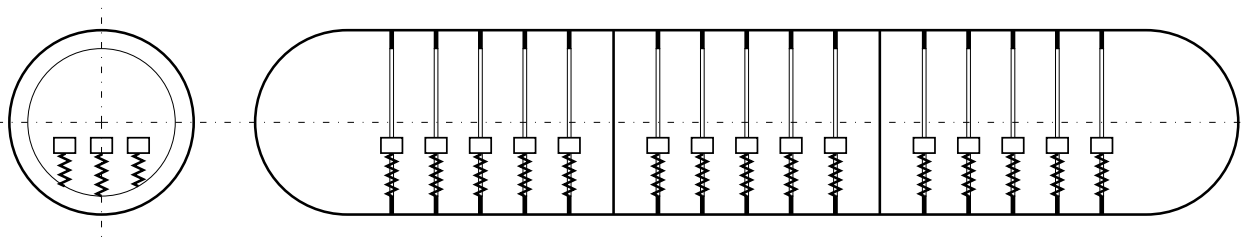


Figure 2. Schematic diagram of the placement of the spring-mass systems in the pressure hull.

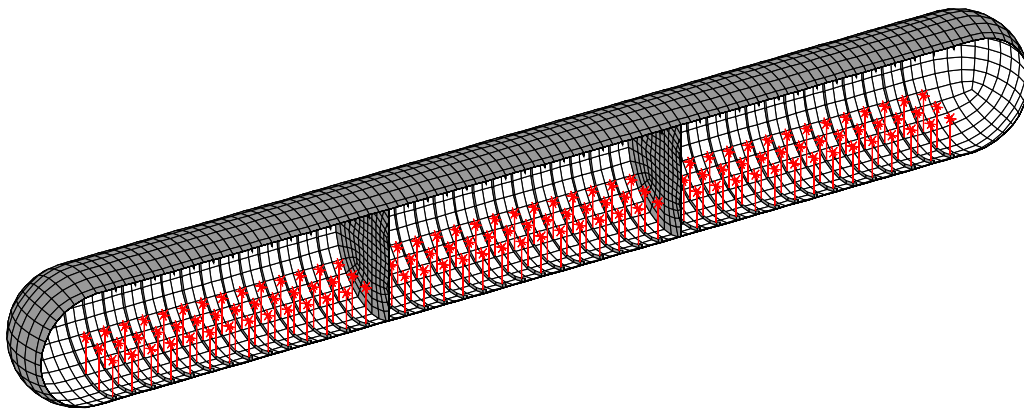


Figure 3. Distribution of the dual spring-mass systems (in red).

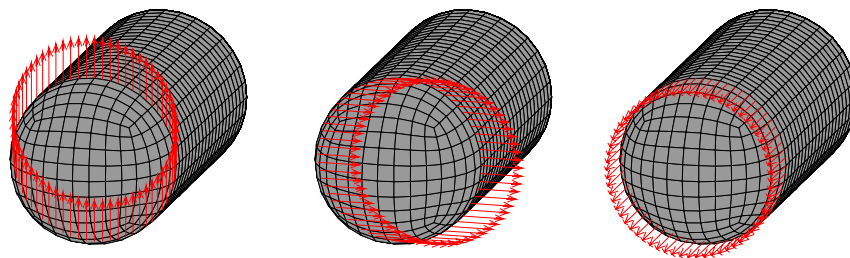


Figure 4. The three load cases for the submerged cylinder in the vertical, transverse and axial directions, respectively.

**K** and **M** are the stiffness and mass matrices of the structure, respectively. The matrices **H** and **G** are the frequency dependent BEM influence matrices obtained through collocation.  $C_{sf}$  and  $C_{fs}$  are the acoustic-structural coupling matrices and are related by  $C_{sf} = C_{fs}^T \Theta$ , where  $\Theta$  is the boundary mass matrix. **p** and **u** are respectively the vectors with the nodal values for pressure and displacement.  $f_s$  and  $f_f$  are the nodal structural forces and the forces due to fluid loading, respectively.  $\omega$  is the angular frequency and  $i$  is the imaginary unit. The sound power is computed using

$$P = \frac{1}{2} \Re \{ \mathbf{p}^T \Theta \mathbf{v}_f^* \} \quad (2)$$

where  $\mathbf{v}_f$  is the fluid particle velocity at the wet surface of the structure.

The force acting on the submerged structure was modelled as a ring-force of 1 N magnitude at the aft of the pressure hull. Figure 4 illustrates the three load cases acting in the vertical, transverse and axial directions, respectively. In a more realistic case, the excitation would be a combination of the three load cases shown in Figure 4. However in this work, the three load cases are considered separately to study the more basic effects of internal mass isolation.

The dimensions and material properties of the hull as well as the fluid parameters are listed in Table 1. The hull parameters were chosen similar to those used previously (Caresta and Kessissoglou, 2009; Merz et al., 2009). The displaced water has a mass of 1637 tonnes. The mass of the hull, bulkheads and ring stiffeners is approximately 430.5 tonnes and the combined mass of the spring-mass systems equals 409.5 tonnes, which is equivalent to 25% of the total mass of the submarine. The difference of 797 tonnes required for neutral buoyancy is distributed evenly over the hull, bulkheads and stiffeners, which is equivalent to increasing the density of steel by 185%. A more complex distribution of this remaining mass has not been considered since internal mass isolation is the primary interest of this work.

**Table 1.** Data for the submerged pressure hull with internal structures

Parameter	Value	Unit
Speed of sound in water	1500	m/s
Density of water	1000	kg/m <sup>3</sup>
Density of steel	7860	kg/m <sup>3</sup>
Added mass to hull, bulkheads, stiffeners	14550	kg/m <sup>3</sup>
Length of hull (without end caps)	45	m
Diameter of hull	6.5	m
Thickness of hull, bulkheads	0.04	m
Thickness of stiffeners	0.08	m
Depth of stiffeners	0.15	m
Loss factor of hull, bulkheads, stiffeners	0.02	-
Mass of spring-mass system	3250	kg
Number of spring-mass systems	126	-
Mounting frequency (flexible side)	5	Hz
Mounting frequency (rigid side)	500	Hz
Loss factor of spring-mass systems	0.1	-

## RESULTS AND DISCUSSION

In order to observe the effect of the rigid and flexible mounted masses, the radiated sound power is computed for the three load cases in a range of 1 to 100 Hz in steps of 0.5 Hz. The computed sound power presented in the following figures is normalised to the dipole sound power shown in Figure 5. Sound radiation due to a point force in the fluid is an important reference across the frequency range, with well-established characteristics (Ross, 1987). It defines the radiation that would exist

due to point excitation if the hull were compact and behaved as an inert body. It is a valuable check on the efficacy of numerical models at very low frequencies. The effects of the hull dynamic response can be seen clearly as an enhancement or reduction of the radiated sound field.

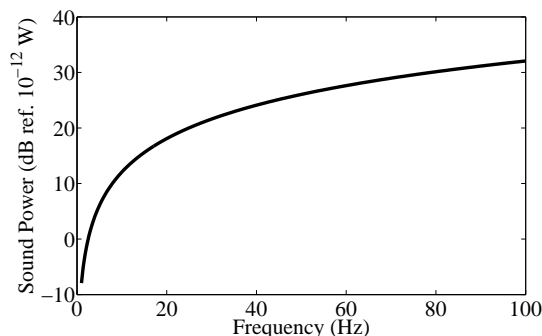


**Figure 5.** Radiated sound power from a dipole.

Figure 6 compares the response of the cylinder with fully isolated spring-mass systems to that of a cylinder without spring-mass systems, which is no longer neutrally buoyant. For the vertical and transverse excitation cases, the peaks of the radiated sound power correspond to radiation from the bending modes of the hull ( $n = 1$  circumferential modes). For the axial excitation case, the peaks correspond to the breathing ( $n = 0$  circumferential) modes of the hull. While higher order modes may also have been excited, no significant contribution to the radiated sound power can be observed from the results. This observation agrees well with the results reported in Ref. (Caresta and Kessissoglou, 2009). Results for the hull with and without internal masses above the resonant frequency of the spring-mass systems at 5 Hz shows that the added internal masses effectively ‘disappear’ and no longer affect the overall system response.

Figure 7 presents the radiated sound power for various degrees of isolation of the internal masses for the vertical, transverse and axial load cases. In Figure 7, the results for 100% isolated correspond to the case where 100% of the internal mass is flexibly mounted. Similarly, the results for 0% isolated correspond to the case where 100% of the internal mass is rigidly attached to the pressure hull. For the transverse excitation case, the internal mass isolation has a minimal effect on the sound power. This is attributed to the fact that under transverse excitation, the internal mass has very little effect on the operational deflection shapes of the fluid-loaded cylinder. For vertical and axial excitation, the interaction between spring-mass systems and the cylinder increases notably. The greatest effect can be observed for axial excitation where the first two axial resonances at approximately 22 and 40 Hz are shifted towards higher frequencies as more internal mass is isolated. In addition to the shift of the resonances to higher frequencies, the peaks of the radiated sound power become broader, which corresponds to increased radiation damping of the fluid-loaded hull. The breathing modes become more dominant because there is less rigidly attached internal mass, thus resulting in greater axisymmetry of the total mass distribution of the hull.

For the case of vertical excitation, a significant effect on the radiated sound power can be observed at around 24 Hz. This effect is due to the coupling of the axial and radial motion of the pressure hull as a result of the asymmetry introduced by the eccentric masses. Figure 8 shows the operational deflection shapes of the pressure hull with internal masses for vertical excitation at 24 Hz. For 100% internal mass isolation corresponding to fully isolated spring-mass systems, it can be seen that the internal masses do not deflect since 24 Hz is well

above the mounting frequency of 5 Hz. For 50% internal mass isolation, the rigidly mounted portion of the internal mass is forced to move with the pressure hull thus significantly affecting the deflection shape. Figure 9 shows the operational deflection shapes of the pressure hull with internal masses for transverse excitation at the same frequency of 24 Hz. The effect of the rigidly attached portion of the internal mass on the global deflection shape is small, which results in a small effect on the radiated sound power.

The propulsion system includes components such as diesel engines, generators, the main motor, gearboxes and propeller-shafting system, which account for a large amount of the total mass of a submarine. This machinery is installed in the aft compartment of a submarine and is isolated from the hull to avoid structure-borne noise transmission and radiated sound. Figure 10 shows the effect of mass isolation in the aft compartment only of the pressure hull while the mass in the other two compartments is rigidly attached to the hull. The most significant effect is observed for vertical excitation for frequencies above 50 Hz, where the radiated sound power for rigidly attached internal masses only is up to 5 dB higher than for isolation of the masses in the aft compartment. The opposite effect is observed under axial excitation. The breathing mode resonant frequencies, as well as the mode radiation efficiencies, increase when mass is removed for the first two axial resonances at 24 and 42 Hz. Internal mass isolation in the aft compartment of the pressure hull reduces sound radiation by the hull  $n = 1$  bending modes but increases sound radiation by the hull  $n = 0$  breathing modes.

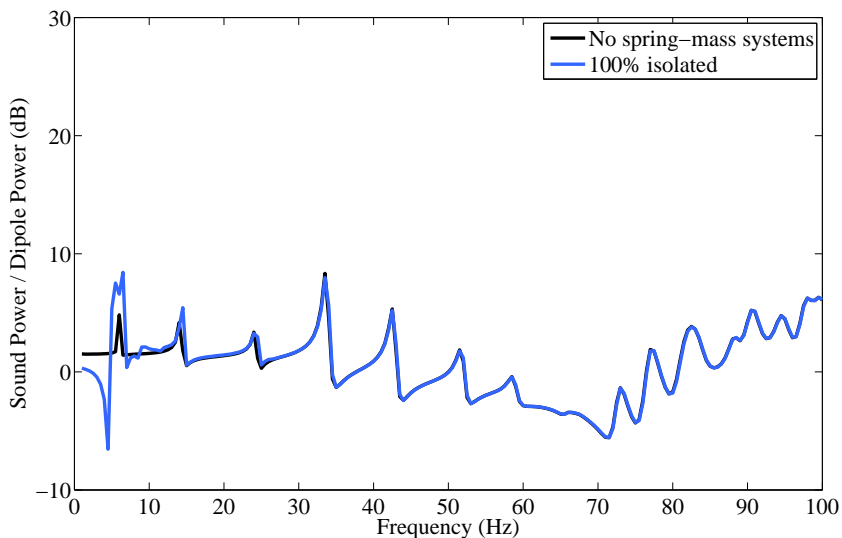
## CONCLUSIONS

A 3D computational model has been developed to study the effects of internal mass isolation on the sound radiation from a submerged pressure hull. A significant portion of the total mass of a submarine due to onboard machinery is isolated from the pressure hull and does not contribute to the effective mass for frequencies approximately three times greater than the natural frequency of the mounting systems. The internal masses were modelled as dual spring-mass systems that could be flexibly or rigidly mounted on the hull. Three load cases corresponding to a ring force acting at the aft of the pressure hull in the vertical, transverse and axial directions were considered. Results showed that varying the degrees of internal mass isolation can have a significant effect on the global hull modes and consequently on the radiated sound power.

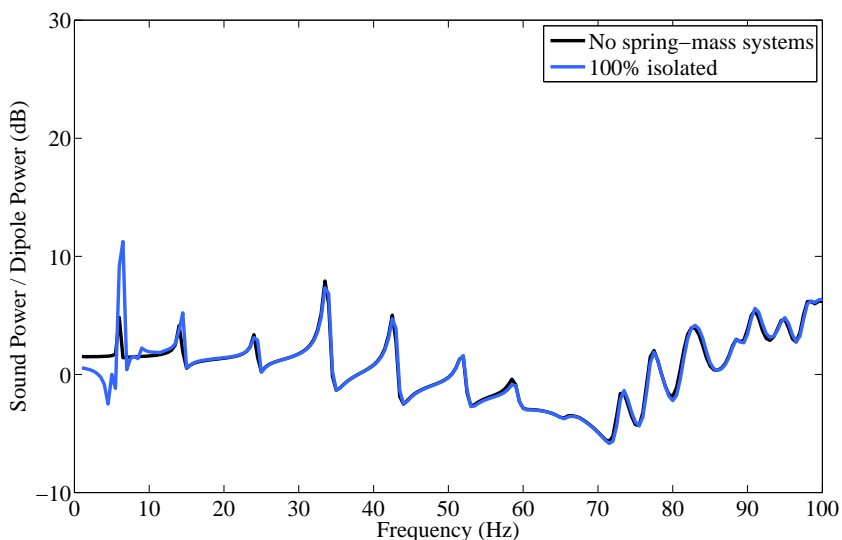
## REFERENCES

- ANSYS (2009). *Theory Reference for the Mechanical APDL and Mechanical Applications*. Release 12.1. ANSYS Inc. Canonsburg, PA, USA.
- Caresta, M and Kessissoglou, NJ (2009). “Structural and acoustic responses of a fluid-loaded cylindrical hull with structural discontinuities”. *Applied Acoustics* 70, pp. 954–963.
- Kinns, R and Faulder, B (1992). “Design of a Low Noise Propulsion Diesel Installation”. *INEC 92: Solutions to the Challenge of a New Defence Environment*. Ed. by R Bufton, A Evripidou, and P Yakimiuk. The Institute of Marine Engineers. Plymouth, UK: Marine Management Ltd, pp. 207–214.
- Marburg, S and Amini, S (2005). “Cat’s eye radiation with boundary elements: comparative study on treatment of irregular frequencies”. *Journal of Computational Acoustics* 13, pp. 21–45.
- Marburg, S and Schneider, S (2003). “Influence of element types on numeric error for acoustic boundary elements”. *Journal of Computational Acoustics* 11, pp. 363–386.

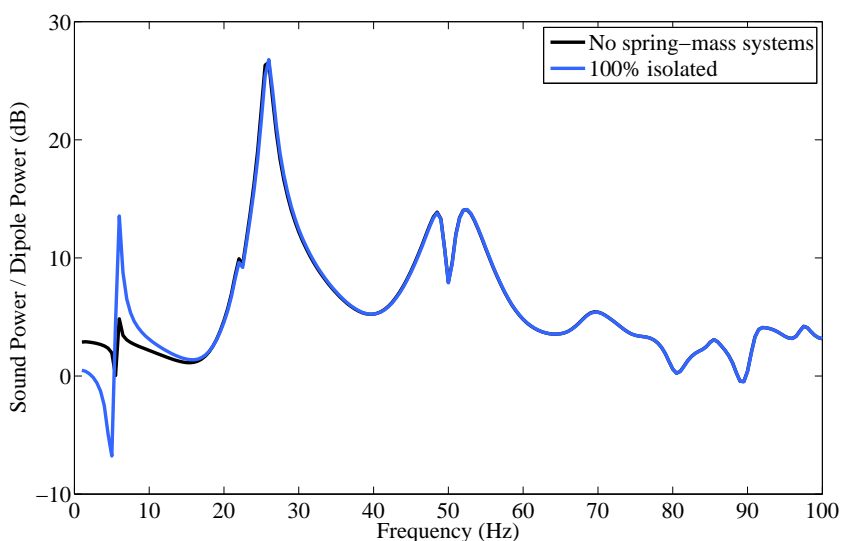
- Merz, S, Kinns, R, and Kessissoglou, NJ (2009). “Structural and acoustic responses of a submarine hull due to propeller forces”. *Journal of Sound and Vibration* 325, pp. 266–286.
- Miller, R (2001). “Acoustic Interactions with Submerged Elastic Structures, Part II”. Ed. by A Guran, G Maugin, J Engelbrecht, and M Werby. Singapore: World Scientific Publishing Company. Chap. The Finite Element/Boundary Element Approach to the Radiation and Scattering of Submerged Shells Including Internal Structure or Equipment, pp. 278–328.
- Pan, X, Tso, Y, and Juniper, R (2008). “Active control of radiated pressure of a submarine hull”. *Journal of Sound and Vibration* 311, pp. 224–242.
- Peters, H, Marburg, S, and Kessissoglou, N (2012). “Structural-acoustic coupling on non-conforming meshes with quadratic shape functions”. *International Journal for Numerical Methods in Engineering* 91(1), pp. 27–38.
- Ross, D (1987). *Mechanics of Underwater Noise*. Los Altos, California, USA: Peninsula Publishing.



(a) Vertical excitation

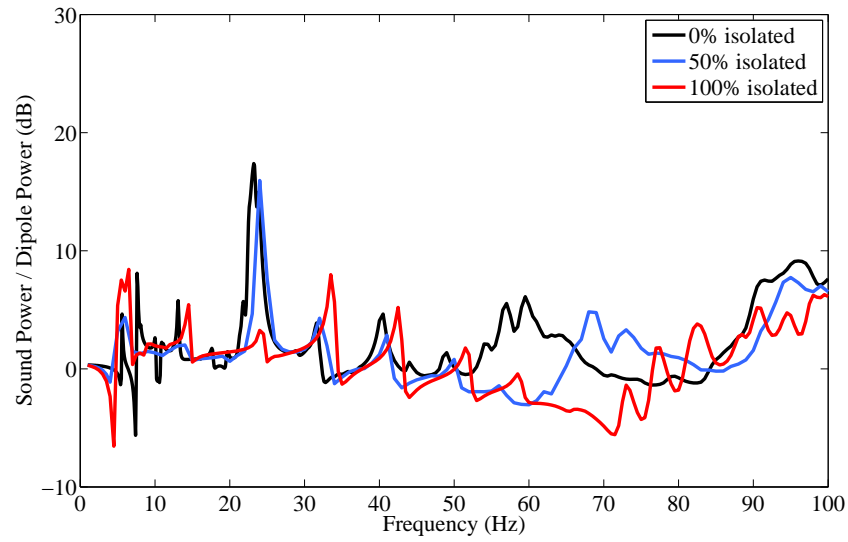


(b) Transverse excitation

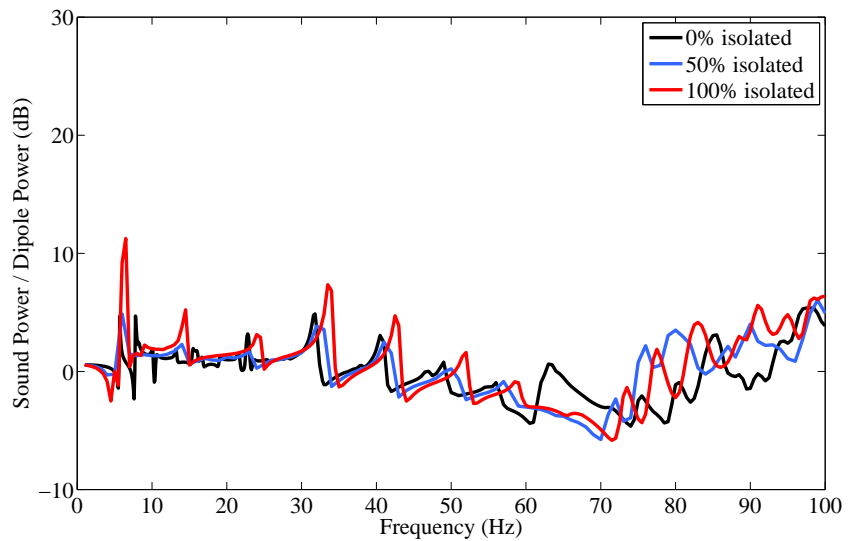


(c) Axial excitation

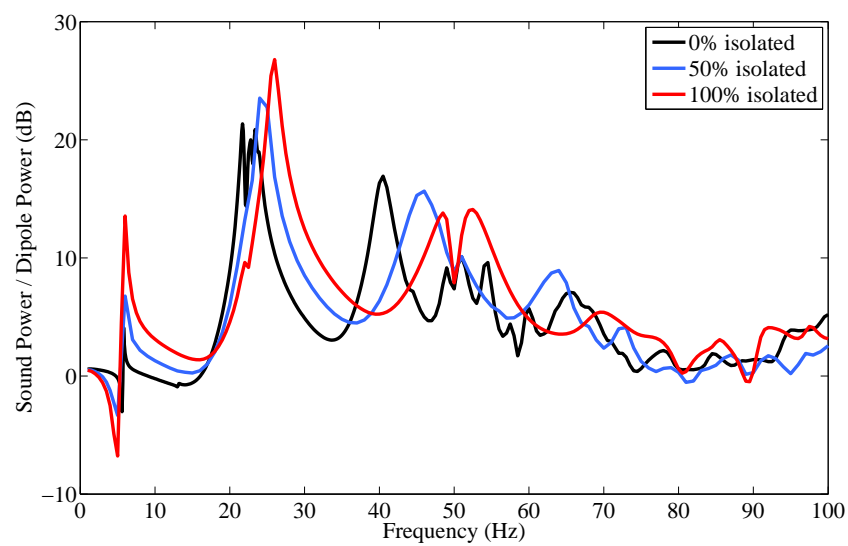
Figure 6. Normalised sound power with and without fully isolated spring-mass systems.



(a) Vertical excitation

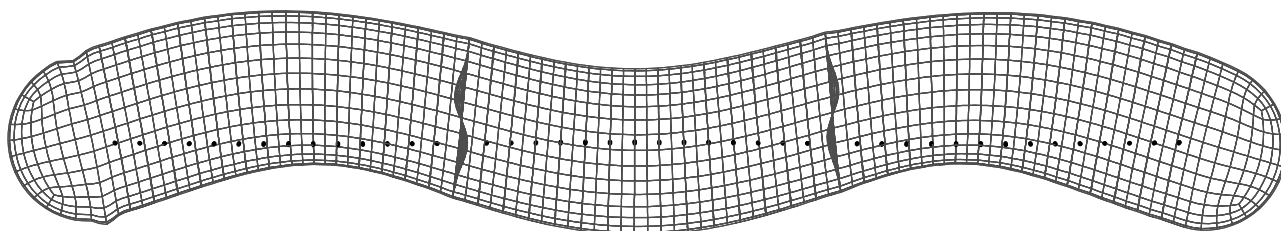


(b) Transverse excitation

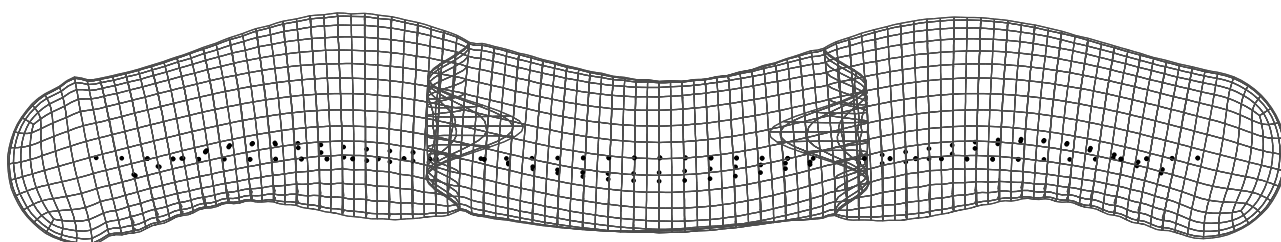


(c) Axial excitation

**Figure 7.** Normalised sound power for pressure hull with 0, 50 and 100% internal mass isolation.

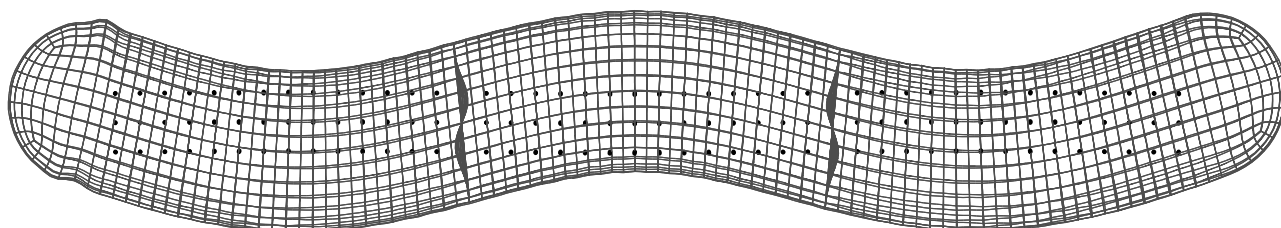


(a) 100% of internal mass isolated from pressure hull

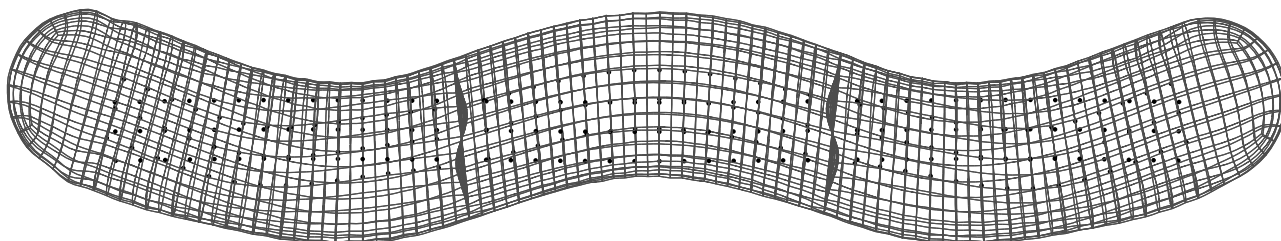


(b) 50% of internal mass isolated from pressure hull

**Figure 8.** Operational deflection shape of the pressure hull with internal masses for vertical excitation at 24 Hz.

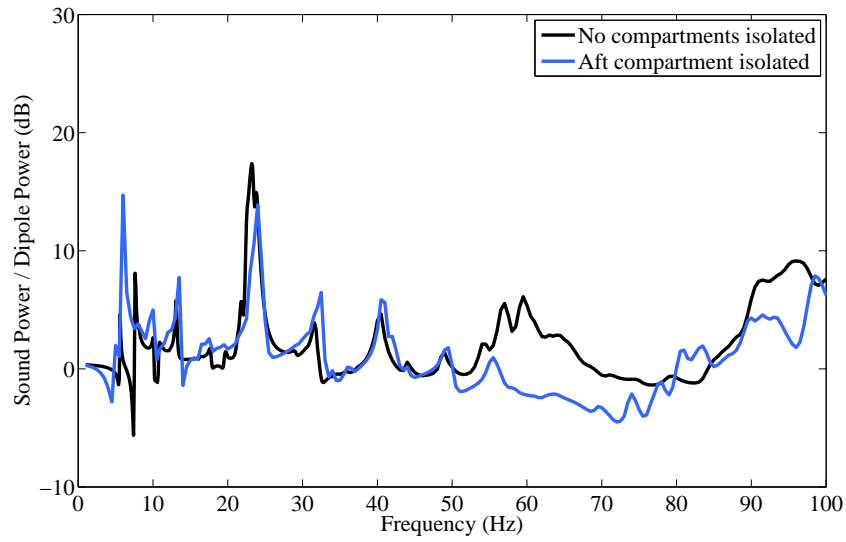


(a) 100% of internal mass isolated from pressure hull

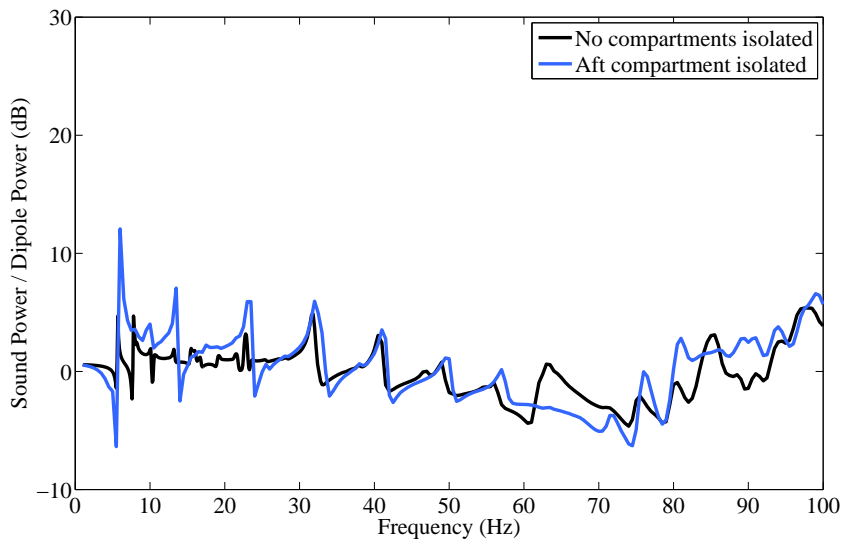


(b) 50% of internal mass isolated from pressure hull

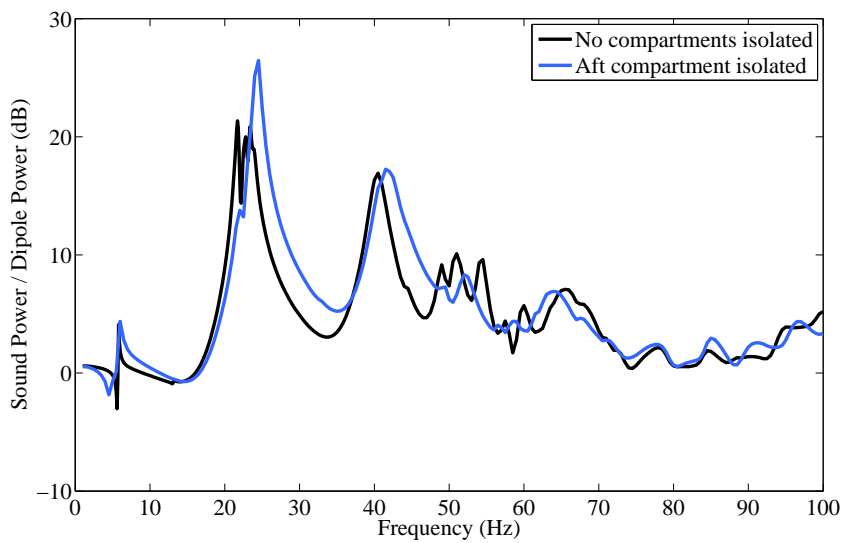
**Figure 9.** Operational deflection shape of the pressure hull with internal masses for transverse excitation at 24 Hz.



(a) Vertical excitation



(b) Transverse excitation



(c) Axial excitation

**Figure 10.** Effect of mass isolation in the aft compartment only on the normalised sound power.